Journal of Controlled Release 160 (2012) 618–629

Contents lists available at SciVerse ScienceDirect

Journal of Controlled Release

journal homepage: www.elsevier.com/locate/jconrel

Novel cathepsin B-sensitive paclitaxel conjugate: Higher water solubility, better efficacy and lower toxicity

Liang Liang [1], Song-Wen Lin [1], Wenbing Dai, Jing-Kai Lu, Ting-Yuan Yang, Yu Xiang, Yang Zhang, Run-Tao Li *, Qiang Zhang **

State Key Laboratory of Natural and Biomimetic Drugs, School of Pharmaceutical Sciences, Peking University, Beijing 100191, China

ARTICLE INFO

Article history:
Received 5 September 2011
Accepted 26 February 2012
Available online 3 March 2012

Keywords:
Paclitaxel
Pegylated
Cathepsin B-sensitive
Conjugate
Anti-tumor effect

ABSTRACT

In order to realize the targeted delivery of paclitaxel (PTX) to tumor through an environment-sensitive mechanism, increase its solubility in water and reformulate without toxic excipients, a novel PTX conjugate, PEG–VC–PABC–PTX was designed and synthesized in this study, using *p*-aminobenzylcarbonyl (PABC), a spacer, and valine–citrulline (VC), a substrate of cathepsin B (C_B), to link polyethylene glycol (PEG) and PTX. Pegylated PTX (PEG-PTX) which was synthesized and Taxol formulation were prepared as controls. The conjugates were purified and characterized by melting points, ^{1}H-NMR, ESI-MS or MALDI-TOF-MS. The two conjugates were similar in particle size, water solubility and their effects on MCF-7 cell line in vitro, and both of them induced no obvious toxicity in vivo. The release of PTX from PEG-PTX was faster due to its ester bond, while PEG–VC–PABC–PTX was proved to be C_B-sensitive in terms of PTX release and its effect on cell cycle. Additionally, PEG–VC–PABC–PTX exhibited significant effects of antitumor, anti-angiogenesis and anti-proliferation in vivo, while the control conjugate was almost inefficacious at the same in vivo test. On the other hand, PTX conjugates demonstrated a thousand-time or more improvement in water solubility compared to PTX, suggesting a very easy way in the preparation and use of its injection. Without involvement of Cremophore EL and ethanol, the PTX conjugate will guarantee less adverse effects as frequently reported for Taxol formulation. Taxol formulation had a higher cytoxicity in vitro than PEG–VC–PABC–PTX likely because of toxic additives. Importantly, the C_B-sensitive conjugate indicated a similar in vivo efficacy with the Taxol control, but much lower in vivo toxicity at the same doses evidenced by body weight, animal status, liver toxicity and blood count. Moreover, at the tolerant dose, this novel conjugate exhibited significantly better antitumor effect than that of Taxol formulation. In general, the PEG–VC–PABC–PTX conjugate designed in this study demonstrated significant advantages in terms of high water solubility, no toxic surfactant or organic solvent, tumor environment-sensitivity and high therapeutic index.

1. Introduction

Cancer is a leading cause of death worldwide: it accounted for 7.9 million deaths (around 13% of all deaths) in 2007. Still, deaths from tumors worldwide are supposed to rise continuously, with an estimated 12 million deaths in 2030 [1]. However, the lack of tumor-specific agents is a long-standing problem faced in cancer treatment. Chemotherapeutics kill cancer cells, and cause a number of undesirable severe side effects due to their non-specific distribution in vivo. Additionally, there is a great challenge in terms of solubilizing the water-insoluble anticancer agent, like paclitaxel (PTX) [2]. Therefore, it is imperative to find a new kind of agent which is water-soluble and specifically active at tumor site.

PTX, isolated from the trunk bark of the Pacific Yew tree, *Taxus brevifolia* [3], is a potent inhibitor of cell replication which was used in the treatment of various cancers including breast and ovarian cancer [4]. However, PTX suffers from significant drawbacks such as aqueous insolubility and dose-limiting toxicity at clinically administered doses [5]. Therefore, in Taxol formulation presently available in the market, PTX needs to be formulated with surfactant Cremophor EL and ethanol. However, Cremophor EL was reported to induce severe toxicities to patients such as hypersensitivity after systemic administration [6,7].

The idea of covalently attaching chemotherapeutic agents to a water-soluble polymer was first proposed by Ringsdorf in the mid-1970s [8]. Since then, accompanied by the development of synthetic and natural polymers, it is becoming a fast-growing field. Such conjugates were developed pre-clinically in 1980s and started to enter the clinical pipeline in the 1990s [9]. For instance, the poly(L-glutamic acid)-paclitaxel conjugate (PG-PTX, coded as CT-2103), showed satisfactory safety and efficacy through the Phases I, II and III studies

* Corresponding author.
** Corresponding author. Tel./fax: +86 10 82802791.
E-mail addresses: lirt@bjmu.edu.cn (R.-T. Li), zqdodo@bjmu.edu.cn (Q. Zhang).
[1] These authors contributed equally to this work.

0168-3659/$ – see front matter © 2012 Elsevier B.V. All rights reserved.
doi:10.1016/j.jconrel.2012.02.020

[10–13]. Other polymer-drug conjugates under development include hydroxypropyl methacrylate (HPMA) copolymer-doxorubicin (coded as PK1, PK2), HPMA copolymer-diamino-cyclohexane (DACH)-platinate (coded as AP5346) and PEG-camptothecin etc. [14]. Polyethelene glycol (PEG) is a hydrophilic polymer approved by FDA and used in pharmaceutical industry for many years as an excipient which shows little toxicity and immunogenicity [15]. In the past forty years, several antitumor agents, such as proteins, peptides and low molecular weight drugs, have been considered for PEGylation [16,17].

However, the concept of linking chemotherapeutic agents to water-soluble polymer is challenged greatly by the fact that polymer like PEG may not be cleavable from the conjugate, even in tumor tissue, led to obvious decrease of the antitumor effect [16]. Whereas, tumor environment-sensitive drug delivery system, which is currently in rapid development, may provide a novel strategy to overcome the obstacles for both drug solubility and site-specific delivery of chemo-drugs [18,19]. In such circumstances, a special linker, sensitive to the pH condition or enzyme system of tumor tissue, may be used to connect the chemotherapeutic agent and the water-soluble polymer, ensuring the drug solubility in water and also the drug release in time from the conjugate at the tumor site [20–23].

Cathepsin B (C_B) is a 30 KDa lysosomal cysteine protease from a family of 11 cysteine proteases [24,25]. In many kinds of cancer, cathepsin B acts as an important proteinase of matrix materials so that tumor cells can actively invade and metastasize [26,27]. It is never found extracellularly, except in pathological conditions such as tumors or in the areas of tissue destruction in rheumatoid arthritis [28]. The general substrates of cathepsin B include valine–citrulline and phenylalanine–arginine [29]. It was reported that some antibody-drug conjugates using the protease-sensitive dipeptide as well as some kind of spacer as the linker showed efficient release of drug in tumor tissues [30].

The purpose of this study is to obtain a water-soluble and tumor environment-sensitive delivery system of PTX through PEGylation as well as the introduction of C_B-sensitive linker with additional spacer, in the hope of that it will exhibit significant advantages over PTX or Taxol formulation in terms of higher water solubility, no toxic surfactant or organic solvent involvement, tumor environment-sensitivity and higher therapeutic index. So, a novel paclitaxel conjugate was synthesized here by using valine–citrulline dipeptide (Val–Cit, or VC), a substrate of C_B, and *p*-aminobenzylcarbonyl (PABC), a spacer, to link PEG and paclitaxel. The PEGylated PTX (PEG-PTX) and the Taxol formulation were used as the controls. For the proof of concept, PEG–VC–PABC–PTX conjugate was synthesized, characterized and evaluated in vitro and in vivo.

2. Material and methods

2.1. Materials

Diisopropylethylamine (DIEA), 2-ethoxy-1-ethoxycarbonyl-1, 2-dihydroquinoline (EEDQ), *N*-hydroxysuccinimide (HOSu), polyethylene glycol monomethyl ether 5000 ($MPEG_{5000}$), *p*-aminobenzyl alcohol (PABOH) and *p*-nitrophenyl (PNP) chloroformate were purchased from Alfa Aesar (Tianjin, China). L-citrulline (L-Cit), 9-fluorenylmethyloxycarbonyl-L-valine (Fmoc-Val), 4-dimethylaminopyridine (DMAP), 1,2-dimethoxyethylene (DME), tetrahydro furan (THF), 1-Ethyl-3-(3-dimethyllaminopropyl)carbodiimide hydrochloride (EDC·HCl), Succinic anhydride, 1,8-Diazabicyclo[5.4.0]undec-7-ene (DBU) and dicyclohexylcarbodiimide (DCC) were obtained from Bo-Mai-Jie Co., Ltd. (Beijing, China). Cathepsin B (C_B) and sulforhodamine B (SRB) were from Sigma Aldrich (St. Louis, MO, USA). Paclitaxel (PTX) was the product of Mei-Lian Co., Ltd. (Chongqing, China). Cremophor EL was purchased from BASF Corporation of Germany (Local Agent in Shanghai, China). Cell culture media DMEM, penicillin streptomycin, and fetal bovine serum were from GIBCO. CD31 and Ki67 were purchased from Abcam. All other chemicals were of analytical or HPLC grade.

2.2. Synthesis of MPEG-$COCH_2CH_2CO$-2′-PTX conjugate (PEG-PTX)

Melting points were determined on X4 microscope. ^{1}H NMR spectra were recorded on a Bruker AVANCE^{III} 400 (400 MHz) instrument at room temperature, with $CDCl_3$ as solvent and TMS as internal reference [6]. ESI-MS spectra were performed on a MDS SCIEX QSTAR spectrometer. On an AXIMA-CFR Plus spectrometer with a nitrogen laser (337.1 nm), MALDI-TOF-MS spectra were obtained in positive ion and linear mode with an acceleration voltage of 20 kV and averaged over 100 laser shots. Each spectrum was externally calibrated with insulin at m/z 2867.80, 5534.59 and 11468.17 respectively providing mass measurement accuracies of approximately 50 ppm across the 1 kDa ~12 kDa mass range.

2.2.1. MPEG-$COCH_2CH_2COOH$

$MPEG_{5000}$ (20 g, 4 mmol) was added to toluene (100 mL) and refluxed for 1 h to remove water. After cooling, toluene was evaporated and the residue was dissolved in $CHCl_3$ (100 mL). Succinic anhydride (2.00 g, 20 mmol) and pyridine (1 mL) were added and the mixture was refluxed for 48 h. $CHCl_3$ was evaporated and distilled water (150 mL) was added. The mixture was filtered, and the filtrate was extracted with $CHCl_3$ (100 mL × 3). The combined organic layers were washed with brine (100 mL × 2), dried over anhydrous Na_2SO_4, filtered and concentrated under reduced pressure. Ether was added, and the resulting white solid was collected by filtration, washed with ether, and dried in vacuo (15.10 g, 74%). The product was characterized by ^{1}H NMR and MALDI-TOF-MS.

2.2.2. MPEG-$COCH_2CH_2CO$-2′-PTX

MPEG-$COCH_2CH_2COOH$ (0.56 g, 0.11 mmol) was added to toluene (10 mL) and the mixture was refluxed for 1 h to remove water. Toluene was then evaporated and the residue was dissolved in CH_2Cl_2 (10 mL). EDC·HCl (0.038 g, 0.20 mmol) was added and the mixture was stirred at 0 °C for 30 min. PTX (0.086 g, 0.10 mmol), DIEA (33 μL, 0.20 mmol) and DMAP (1.2 mg, 0.01 mmol) was added, and the mixture was warmed to room temperature and stirred for another 24 h. Then the mixture was washed with brine (10 mL), and the aqueous layer was extracted with CH_2Cl_2 (10 mL). The combined organic layers were dried over anhydrous Na_2SO_4, filtered and evaporated. The residue was purified by column chromatography ($CHCl_3$:CH_3OH = 40:1 then 10:1) to afford the product as a white foamed solid (0.54 g, 91%). The product was characterized by MALDI-TOF-MS.

2.3. Synthesis of MPEG-$COCH_2CH_2CO$-Val-Cit-PABC-2′-PTX conjugate (PEG–VC–PABC–PTX)

2.3.1. Fmoc-Val-Cit [29]

Fmoc-Val (5.06 g, 14.91 mmol), HOSu (1.72 g, 14.91 mmol) and DCC (3.08 g, 14.91 mmol) were added to THF (50 mL) at 0 °C and the mixture was stirred at room temperature for 16 h, and then filtered and washed with THF. The solvent was removed under reduced pressure, and the resulting glassy solid (Fmoc-Val-OSu) was used without purification in the next step.

Fmoc-Val-OSu (14.91 mmol) in DME (40 mL) was added to a solution of Cit (2.74 g, 1.05 equiv) and $NaHCO_3$ (1.32 g, 1.05 equiv) in water (40 mL). THF (20 mL) was added to aid solubility, and the mixture was stirred at room temperature for 16 h. Aqueous citric acid (15%, 75 mL) was added, and the mixture was extracted with 10% isopropanol/ethyl acetate (100 mL × 3). The combined organic layers were washed with water (150 mL × 3), and the solvents were evaporated. The resulting white glassy solid was added to ether (80 mL).

After sonication and trituration, the white solid product was collected by filtration, washed with ether, and dried in vacuo (4.64 g, 63%). The product was characterized by ^{1}H NMR.

2.3.2. Fmoc-Val-Cit-PABOH [29]

Fmoc-Val-Cit (1.04 g, 2.10 mmol) and PABOH (0.52 mg, 4.20 mmol) in 2:1 CH_2Cl_2/CH_3OH (24 mL/12 mL) were treated with EEDQ (1.04 g, 4.20 mmol). The mixture was stirred in the dark at room temperature for 36 h. The solvents were removed under reduced pressure at 40 °C, and ether (75 mL) was added. The mixture was triturated and sonicated for 5 min and then left to stand for 30 min. The solid was collected by filtration, washed with ether, and dried in vacuo (1.10 g, 82%). The product was characterized by ^{1}H NMR.

2.3.3. Fmoc-Val-Cit-PABC-PNP

A mixture of Fmoc-Val-Cit-PABOH (0.30 g, 0.5 mmol), PNP chloroformate (0.20 g, 1.0 mmol) and pyridine (80 μL, 1.0 mmol) in THF (25 mL) was stirred at room temperature over night. The solvent was evaporated under vacuum and the residue was purified by column chromatography ($CHCl_3$:CH_3OH = 30:1 then 20:1) to afford the product as a pink foamed solid (0.20 g, 52%). The product was characterized by ^{1}H NMR and ESI-MS.

2.3.4. Fmoc-Val-Cit-PABC-2′-PTX

A mixture of Fmoc-Val-Cit-PABC-PNP (0.16 mg, 0.21 mmol), PTX (0.22 mg, 0.25 mmol) and DMAP (0.031 g, 0.25 mmol) in CH_2Cl_2 (20 mL) was stirred at room temperature for 48 h. The solvent was evaporated under vacuum and the residue was purified by column chromatography ($CHCl_3$:CH_3OH = 30:1 then 20:1) to afford the product as a pink foamed solid (0.18 g, 59%). The product was characterized by ^{1}H NMR and ESI-MS.

2.3.5. MPEG-$COCH_2CH_2CO$-Val-Cit-PABC-2′-PTX

MPEG-$COCH_2CH_2COOH$ (0.69 g, 0.14 mmol) was added to toluene (10 mL) and the mixture was refluxed for 1 h to remove water. Toluene was then evaporated and the residue was dissolved in CH_2Cl_2 (10 mL). The resulting solution was cooled to 0 °C, and EDC·HCl (0.047 g, 0.25 mmol) was added. The mixture was stirred for 30 min at 0 °C, and then transferred to a solution of Fmoc-Val-Cit-PABC-2′-PTX (0.18 g, 0.12 mmol) and DBU (37 μL, 0.25 mmol) in THF (8 mL) which was previously stirred for 10 min to remove the Fmoc protective group. After reacting at room temperature for 24 h, the mixture was washed with brine (10 mL), and the aqueous layer was extracted with CH_2Cl_2 (10 mL). The combined organic layers were dried over anhydrous Na_2SO_4, filtered and evaporated. The residue was purified by chromatography ($CHCl_3$:CH_3OH = 40:1 then 12:1) to afford the product as a white foamed solid (0.23 g, 30%). The product was characterized by MALDI-TOF-MS.

2.4. Solubility test

Excess PTX powder and PTX conjugate prepared in this study were put into three different kinds of medium, pure water, 5% glucose and physiological saline, respectively. Then the test system was shaken at room temperature for 48 h, followed by the centrifugation at 10000 rpm for 10 min. Finally, each supernate was diluted and determined by HPLC [31]. The HPLC assay was conducted using a Phenomenex® C18 column (5 μm, 250 × 4.6 mm) kept at 35 °C and an UV detector set at 232 nm. Acetonitrile and water (53:47, V/V) were used as mobile phase at a flow-rate of 1.0 mL/min.

2.5. Particle size and morphology

The apparent particle sizes of the nanoparticles formed from conjugates were determined by dynamic light scattering (DLS) using Malvern Zetasizer Nano ZS (Malvern, UK) at 25 °C, and the shape and surface morphology of conjugates were investigated by transmission electron microscope (TEM, JEM-1230, JEOL, JAPAN) after negative staining with uranyl acetate solution (1%, w/v).

2.6. Drug release in vitro

The conjugate prepared in this study was incubated in 1 mL DMEM with 10% FBS at 37 °C with shaking (100 rpm). Aliquots of 100 μL of incubation medium were removed at predetermined time points (1, 2, 4, 6, 8, 12, 24 h), and mixed with 2.5 mL methyl-butyl ether in a vortex mixer for 2 min. Then 2 mL supernate was collected and dried in nitrogen at 40 °C. The residue was dissolved in 100μL mobile phase. The supernatant (20 μL) was injected into the HPLC system for drug analysis.

2.7. C_B sensitivity of conjugates

C_B was preincubated in the activation buffer containing 50 mmol/L sodium acetate (pH5.0), 2 mmol/L dithiothreitol (DTT), and 25% (v/v) glycerol for 15 min at 37 °C. The activated C_B solution then was diluted with 2 mL of 25 mM acetate/1 mM EDTA buffer (pH5.0, preincubated at 37 °C) [29]. The final concentration of C_B in this solution was 10 unit/mL. Then conjugate was added to C_B solution. The whole system was incubated at 37 °C for 24 h. The free PTX was detected by HPLC [31]. The HPLC condition was mentioned above.

2.8. Cell culture

Human breast cancer cells MCF-7 (Institute of Material Medical, Chinese Academy of Medical Sciences and Peking Union Medical College, Beijing, China) were employed as an in vitro cell model. The MCF-7 cells were maintained in the DMEM medium with 10% FBS and 1% penicillin–streptomycin solution. The cells were incubated at 37 °C in the humidified environment of 5% CO_2. The medium was replenished every two days until confluence was achieved. The cells were then washed with PBS and harvested with 0.25% trypsin solution. PTX solution (dissolved in DMSO then diluted by DMEM) and conjugate solution (dissolved in water then diluted by DMEM) were used in all the cell tests.

2.9. In vitro cytotoxicity

MCF-7 cells were seeded at a density of 2×10^3 cells/well in a 96-well transparent plate and incubated for 24 h. Then various concentrations of PTX or conjugate solution were added to the medium. After 72 h, the cell viability was determined by the SRB assay [32]. Briefly, the medium was removed, and then cells were fixed with trichloroacetic acid, washed and stained with SRB. The absorbance was measured at 540 nm using a 96-well plate reader (Bio-rad, 680, America). The survival percentages were calculated using the following formula: Survival% = (A540 nm for the treated cells/A540 nm for the control cells) × 100%, where A540 nm is the absorbance value. Each assay was repeated for triplicates. Finally, dose–effect curves were made and IC_{50} values were calculated.

2.10. Cell cycle analysis

Cell cycle perturbations induced by PTX or conjugates were analyzed by propidium iodide (PI) DNA staining. Briefly, exponentially growing MCF-7 cells were treated with 20 nM PTX, 20 nM PEG-PTX and 20 nM PEG–VC–PABC–PTX conjugate for 12 h, with or without C_B, respectively. The MCF-7 cells incubated with DMEM were used as the control. At the end of each treatment, cells were collected after a gentle centrifugation at 1200 rpm for 5 min and then fixed in 70% ethanol for 12 h at 4 °C. Ethanol-suspended cells were diluted

with PBS and then centrifuged at 1200 rpm for 5 min to remove residual ethanol. For cell cycle analysis, the pellets were suspended in 0.5 mL of PBS, and incubated with 1 mg/mL of DNase-free RNase A at 37 °C for 30 min. Then 0.1 ml of 0.1% of Triton X-100 containing 0.02 mg/mL of PI was added. Cell cycle profiles were studied using a FACScan flow cytometer (Becton Dickinson FACSCalibur, Mountain View, CA, USA). The data were analyzed through FCS Express V 3 software. Each assay was repeated for triplicates.

2.11. In vivo anti-tumor efficacy

The 6–8 week old female BALB/c nude mice inoculated with MCF-7 cells (10^6) in the left armpit were used in the studies. All care and handling of animals were performed with the approval of Institutional Authority for Laboratory Animal Care of Peking University. In the comparison test among different PTX conjugates, tumor-bearing nude mice were randomly divided into three groups of 6 mice: 5% glucose solution (control), PEG-PTX and PEG–VC–PABC–PTX. The conjugates in 5% glucose solution were given at a dosage of 10 mg PTX/kg. Administration via tail vein injection was started at day 6 post tumor inoculation when the average tumor size reached 80 mm^3 and continued at days 8, 10, 12 and 14. The tumor size was recorded at days 7, 9, 11, 13 and 15 accordingly. The tumor volume was measured with digital caliper in two dimensions and calculated as follows: $(\text{length}) \times (\text{width})^2/2$ [33]. At the end of the test, tumors were harvested and weighted.

Then PEG–VC–PABC–PTX conjugate at various doses was compared with Taxol formulation (prepared according to the formulation of Taxol), MCF-7 tumor-bearing nude mice were randomly divided into five groups of 6 mice: 5% glucose, Taxol formulation (10 mg/kg), PEG–VC–PABC–PTX (equimolar with 10 mg/kg PTX), PEG–VC–PABC–PTX (equimolar with 15 mg/kg PTX) and PEG–VC–PABC–PTX

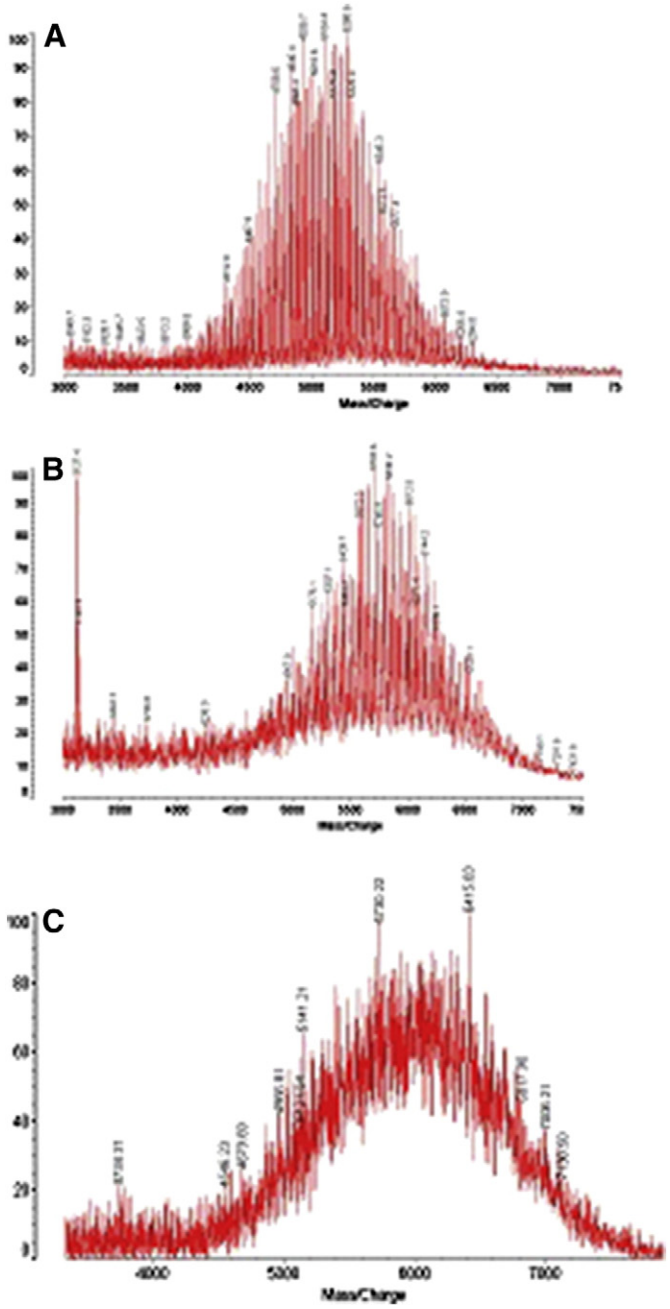

Fig. 1. MALDI-TOF spectra of MPEG-$COCH_2CH_2COOH$ (a), PEG-PTX (b), and PEG–VC–PABC–PTX (c).

(equimolar with 20 mg/kg PTX). The manipulation was the same as mentioned above, except that tumor size was recorded until day 17.

2.12. Effect on the angiogenesis, cell proliferation and toxicity in vivo

The tumors of different treatment groups were embedded and prepared into serial sections (4 μm thick). For analysis of tumor vasculature, CD31 antibody (Abcam, 1:200) was used for microvessel staining. For cell proliferation analysis, sections were incubated with Ki-67 antibody (Abcam, 1:200). The method of immunohisto-chemistry used here was basically according to reference [34].

At end point, 20 μl blood sample was collected from retro-orbital sinus for each mouse. The blood count was determined by a MEK-6318K Hematology Analyzer (Nihon Kohden, Japan) to preliminarily

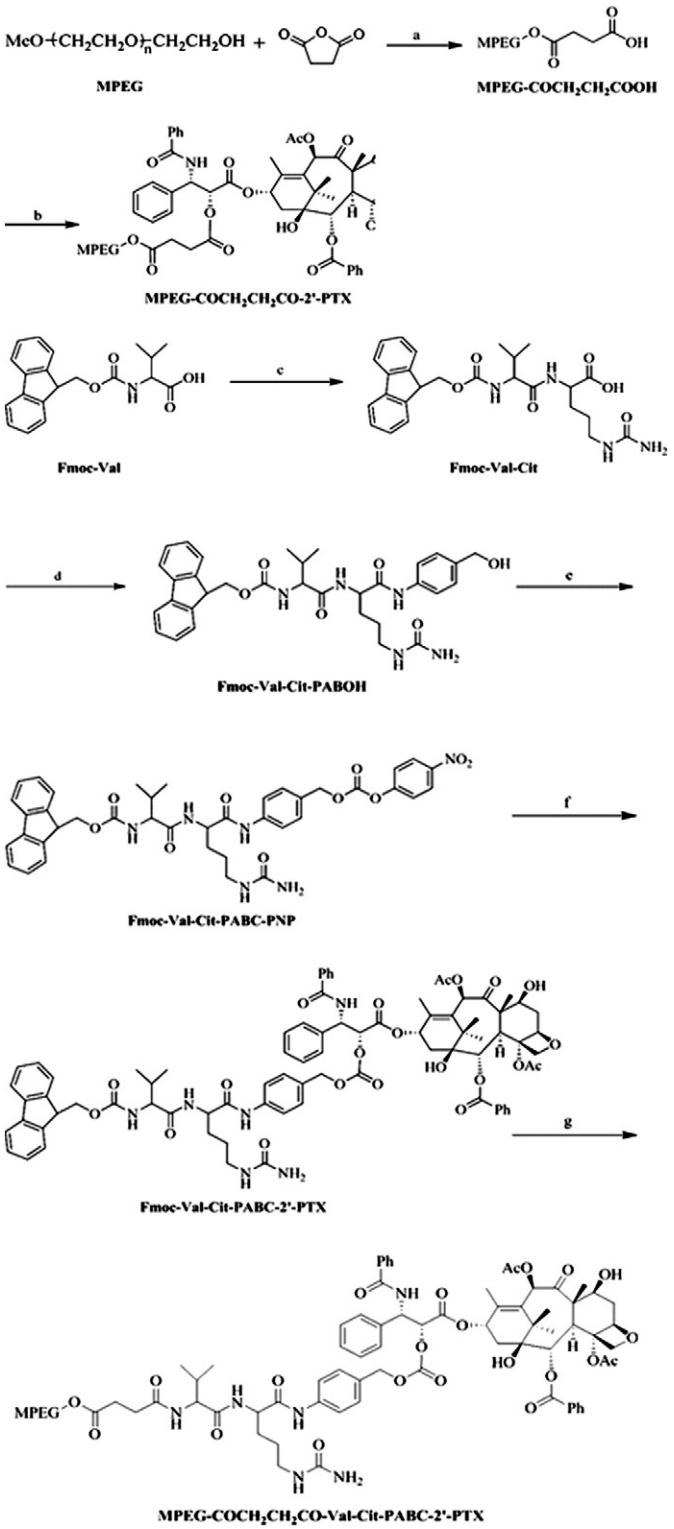

Scheme 1. Synthetic routes. Reagents and conditions: (a) pyridine, $CHCl_3$, reflux; (b) PTX, EDC·HCl, DIEA, DMAP, CH_2Cl_2; (c) i) HOSu, DCC, THF; ii) Cit, $NaHCO_3$, H_2O, DME, THF (d) PABOH, EEDQ, CH_2Cl_2, CH_3OH; (e) PNP chloroformate, pyridine, THF; (f) PTX, DMAP, CH_2Cl_2; (g) i) DBU, THF; ii)MPEG-$COCH_2CH_2$ COOH, EDC·HCl, DIEA, DMAP, CH_2Cl_2.

assess the blood toxicity of PTX and PTX conjugate. Additionally, H&E staining of the liver tissue sections was conducted for the histological study of liver toxicity.

2.13. Data analysis

Data are shown as means ± SD unless particularly outlined. Student's *t*-test or one-way analyses of variance (ANOVA) were performed in statistical evaluation. A p value less than 0.05 was considered to be significant.

3. Results

3.1. Characterization of PEG-PTX

3.1.1. MPEG-$COCH_2CH_2COOH$

The characteristic peaks for MPEG-$COCH_2CH_2COOH$ were found in the ^{1}H NMR spectrum of MPEG-$COCH_2CH_2COOH$. As shown in Fig. 1a, The MALDI-TOF-MS spectrum exhibited the center of the peak at m/z 5100. All these results supported that MPEG had been conjugated with succinic anhydride. ^{1}H NMR (400 MHz, $CDCl_3$): δ 2.60 (m, 4H), 3.38 (s, 3H), 3.46 (t, J = 5.2 Hz, 2H), 3.55 (t, J = 5.2 Hz, 2H), 3.64 (m), 3.82 (t, J = 4.8 Hz, 4H), 4.26 (t, J = 4.8 Hz, 2H).

3.1.2. MPEG-$COCH_2CH_2CO$-2′-PTX

The synthetic route and structure of MPEG-$COCH_2CH_2CO$-2′-PTX are shown in Scheme 1. The MALDI-TOF-MS spectrum exhibited the center of the peak at m/z 5800. All these results supported that MPEG-$COCH_2CH_2COOH$ had been conjugated with PTX successfully. MS (MALDI-TOF): m/z peak at 5700 (Fig. 1b).

3.2. Characterization of MPEG–VC–PABC–PTX

3.2.1. Fmoc-Val-Cit

The structure of Fmoc-Val-Cit was confirmed by the characteristic peaks which were in accordance with that reported in reference [29].^{1}H NMR (400 MHz, DMSO-d_6): δ 0.86 (d, J = 6.8 Hz, 3H), 0.89 (d, J = 6.4 Hz, 3H), 1.36–1.73 (m, 4H), 1.94–2.00 (m, 1H), 2.92–2.97 (m, 2H), 3.92 (t, J = 8.0 Hz, 1H), 4.12–4.31 (m, 4H), 5.36 (br s, 2H), 5.92 (t, J = 4.8 Hz, 1H), 7.31–7.44 (m, 5H), 7.75 (t, J = 7.2 Hz, 2H), 7.90 (d, J = 7.6 Hz, 2H), 8.16 (d, J = 7.2 Hz, 1H), 12.51 (br s, 1H).

3.2.2. Fmoc-Val-Cit-PABOH

The structure of Fmoc-Val-Cit-PABOH was approved by the characteristic peaks which were in accordance with that reported in reference [29]. ^{1}H NMR (400 MHz, DMSO-d_6): δ 0.86 (d, J = 6.8 Hz, 3H), 0.88 (d, J = 6.8 Hz, 3H), 1.37–1.69 (m, 4H), 1.94–2.03 (m, 1H), 2.92–3.05 (m, 2H), 3.93 (t, J = 7.6 Hz, 1H), 4.23–4.44 (m, 6H), 5.09 (t, J = 5.6 Hz, 1H), 5.40 (br s, 2H), 5.97 (t, J = 5.6 Hz, 1H), 7.23 (d, J = 8.4 Hz, 2H), 7.31–7.44 (m, 5H), 7.54 (d, J = 8.4 Hz, 2H), 7.74 (t, J = 7.2 Hz, 2H), 7.89 (d, J = 7.6 Hz, 2H), 8.09 (d, J = 7.2 Hz, 1H), 9.97 (s, 1H).

3.2.3. Fmoc-Val-Cit-PABC-PNP

The characteristic peaks of Fmoc-Val-Cit-PABC-PNP were all observed in the ^{1}H NMR spectrum. The ESI-MS spectrum exhibited the peak at m/z 766.14, 789.10, which corresponds to the $[M+H]^+$ and $[M+Na]^+$, respectively. All these results supported that Fmoc-Val-Cit-PABC-PNP had been obtained. ^{1}H NMR (400 MHz, DMSO-d_6): δ 0.86 (d, J = 6.8 Hz, 3H), 0.88 (d, J = 6.8 Hz, 3H), 1.39–1.69 (m, 4H), 1.97–2.02 (m, 1H), 2.97–3.06 (m, 2H), 3.94 (t, J = 7.6 Hz, 1H), 4.23–4.43 (m, 4H), 5.25 (s, 2H), 5.41 (br s, 2H), 5.98 (t, J = 6.0 Hz, 1H), 7.31–7.77 (m, 13H), 7.89 (d, J = 7.6 Hz, 2H), 8.14 (d, J = 7.6 Hz, 1H), 8.23–8.33 (m, 2H), 10.14 (s, 1H). MS (ESI+): m/z 766.14 $[M+H]^+$, 789.10 $[M+Na]^+$.

Table 1
Solubility of PTX and PTX conjugates in different medium (PTX: mg/mL).

	PTX	PEG-PTX	PEG–VC–PABC–PTX
Water	4.03×10^{-3}	4.33	5.36
Saline	4.26×10^{-3}	3.05	4.13
5% glucose	5.83×10^{-3}	2.43	4.32

Table 2
Apparent particle size of the two conjugates (n = 3).

Group	Particle size (nm)	PDI
PEG-PTX	159.4 ± 5.0	0.223 ± 0.017
PEG–VC–PABC–PTX	122.5 ± 0.4	0.61 ± 0.15

3.2.4. Fmoc-Val-Cit-PABC-2′-PTX

The characteristic peaks of Fmoc-Val-Cit-PABC-2′-PTX were observed in the ^{1}H NMR spectrum. The ESI-MS spectrum exhibited the peak at m/z 1503.81, which corresponds to the $[M+Na]^+$. All these results supported that Fmoc-Val-Cit-PABC-2′-PTX had been obtained. ^{1}H NMR (400 MHz, $CDCl_3$): δ 0.85–0.89 (m, 6H), 1.13 (s, 3H), 1.17 (s, 3H), 1.42–1.92 (m, 12H), 2.04–2.59 (m, 11H), 3.11–3.30 (m, 2H), 3.67 (d, J = 6.8 Hz, 1H), 3.69 (d, J = 5.6 Hz, 1H), 4.09–4.76 (m, 10H), 4.96–5.31 (m, 3H), 5.47 (d, J = 3.6 Hz, 1H), 5.64–5.73 (m, 2H), 5.95 (dd, J = 3.6, 8.8 Hz, 1H), 6.14 (t, J = 8.4 Hz, 1H), 6.27 (s, 1H), 7.11–7.74 (m, 27H), 8.12 (d, J = 7.2 Hz, 2H), 9.25 (br s, 1H). MS (ESI+): m/z 1503.81 $[M+Na]^+$.

3.2.5. MPEG-$COCH_2CH_2CO$-Val-Cit-PABC-2′-PTX

The synthetic route of MPEG-$COCH_2CH_2CO$-Val-Cit-PABC-2′-PTX is presented in Scheme 1. The MALDI-TOF-MS spectrum exhibited

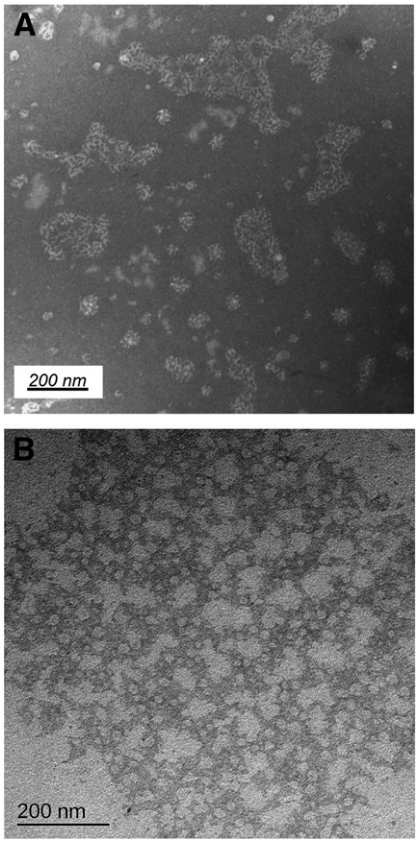

Fig. 2. Transmission electron microscopy image of conjugates suspend in PBS at a concentration of 0.1 mg/mL. A: PEG–VC–PABC–PTX; B: PEG-PTX.

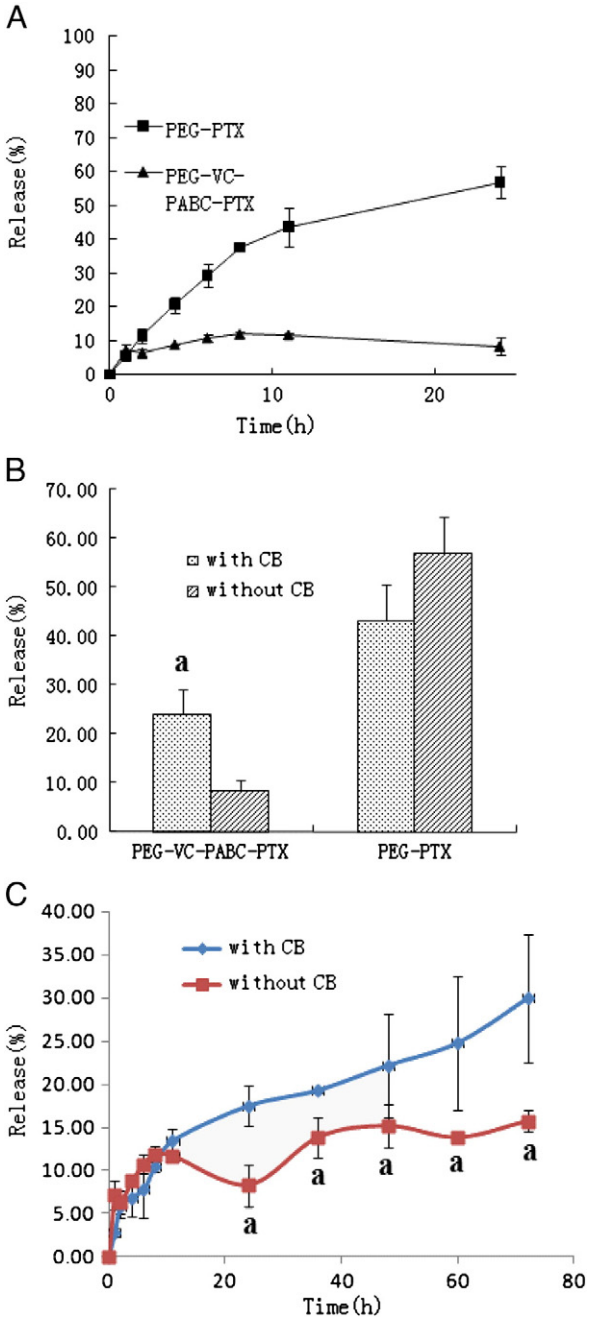

Fig. 3. In vitro release of PTX from each conjugate in DMEM with 10% FBS at 37 °C. A: release curve without C_B; B: C_B-sensitivity test for two conjugates at 24 h; C: C_B-sensitivity test for PEG–VC–PABC–PTX at different time; a: $p<0.01$ versus that without C_B.

the center of the peak at m/z 6100. All these results supported that the conjugate had been obtained successfully. MS (MALDI-TOF): m/z peak at 6100 (Fig. 1c).

From the conjugate structure as well as its molecular weight of 6100, it was clear that one molecule of the conjugate contains only one molecule of PTX. So, the amount of PTX (MW 853) bound to the conjugate was 13.98%. The total synthesis yield of PEG–VC–PABC–PTX was 17.7% based on PTX and calculated from the reaction yield in each of the two steps related.

Table 3
IC_{50} values of PTX conjugates and PTX after incubation with MCF-7 cell for 72 h (Unit: nM, n = 3).

PTX	PEG-PTX	PEG–VC–PABC–PTX
6.38 ± 1.06	40.32 ± 3.39[a]	34.28 ± 3.38[a]

[a] $p<0.0005$ versus PTX.

3.3. Solubility

The solubility of free PTX and two PTX conjugates is shown in Table 1. As been seen, the PTX had a very poor solubility in three commonly-used media. After connection to PEG with or without linker, the solubility of PTX conjugates increased enormously, from the μg/mL to the mg/mL order of magnitude, suggesting a thousand-time or more improvement in solubility. The solubility of two PTX conjugates in different medium was in the same order of magnitude.

3.4. Particle size and morphology

As shown in Table 2, each kind of conjugate possessed an apparent mean particle size in DLS analysis between 100 and 200 nm, with a polydispersity index (PDI) between 0.2 and 0.7. In TEM graph (Fig. 2), the diameter of PEG–VC–PABC–PTX on average was larger than 100 nm also with a rather big fluctuation in particle size. Additionally, the conjugate seemed to form the "nano-aggregate".

3.5. Drug release in vitro

In vitro release profiles of PTX from the two conjugates are shown in Fig. 3A. There was obvious difference in the drug release pattern between the two conjugates. In PEG-PTX group, more than 50% of free PTX was detected in 24 h. While only about 10% of free drug was released from PEG–VC–PABC–PTX conjugate after 24 h test.

3.6. C_B sensitivity of conjugates

The sensitivity of conjugates to C_B was tested here by monitoring the drug released from this conjugate in the presence of C_B, and the data is shown in Fig. 3B and C. In comparison with 8.03% of PTX released from PEG–VC–PABC–PTX conjugate after incubated without C_B at 37 °C for 24 h, 24.06% of PTX was released when C_B was added to the same system. There was a significant difference between the two groups ($p<0.01$), revealing the obvious sensitivity of PEG–VC–PABC–PTX conjugate to C_B. However, PEG-PTX conjugate changed little ($p>0.1$) after C_B was added.

3.7. In vitro cytotoxicity

The cytotoxicities of two PTX conjugates and PTX solution are shown in Table 3. The free drug (PTX) exhibited the highest cytotoxicity as expected. The cytotoxicity of PEG-PTX or PEG–VC–PABC–PTX was much lower than PTX group, indicating the negative effect of chemical linkage at 2′-OH of PTX on their cytotoxicity. There is no significant difference between PEG-PTX group and PEG–VC–PABC–PTX group.

3.8. Cell cycle analysis

A proliferating culture of MCF-7 cells was incubated with 20 nM of PTX or PTX conjugates for 12 h with or without the existence of adscititous C_B. The results are shown in Fig. 4 and Table 4. Based on the antitumor mechanism of PTX, the fraction of cells in G_2-M phase is the most important parameters [35,36].

As shown in Table 4, there was a significant difference between cell group (negative control) and PTX group (positive control) ($p<0.001$), suggesting the feasibility of the methodology. However, the effect of PEG–VC–PABC–PTX and PEG-PTX conjugate on cell cycle was significantly lower than PTX groups. PEG–VC–PABC–PTX

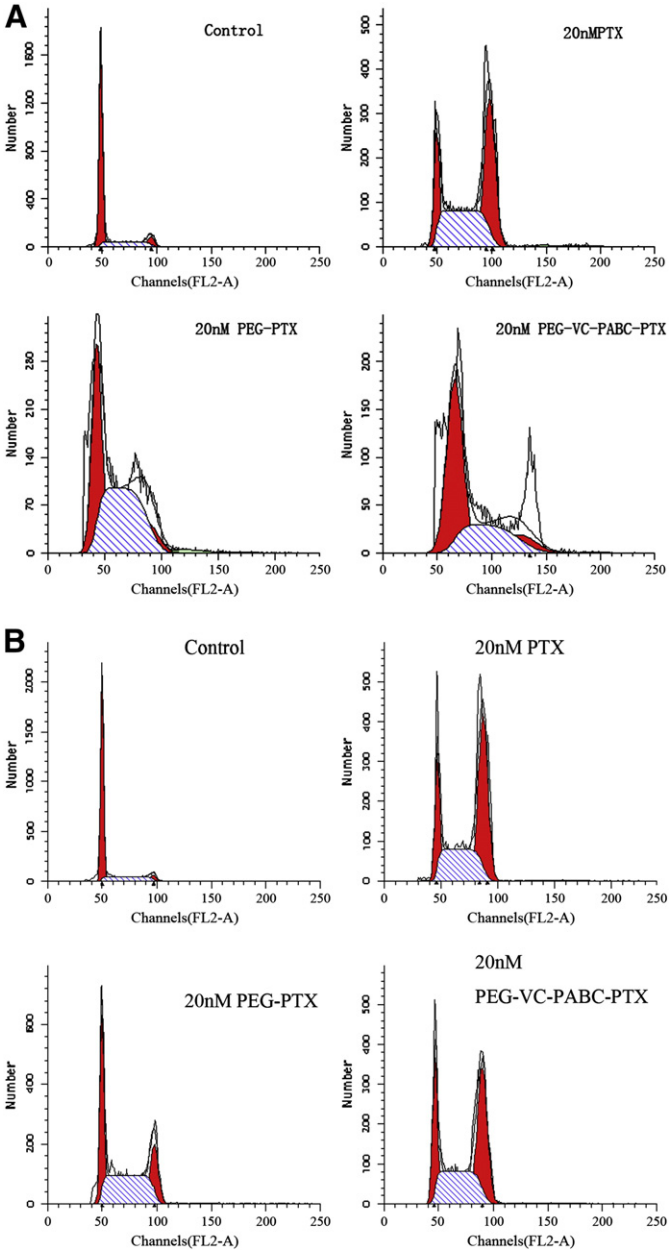

Fig. 4. Effects of different treatments on the cell cycle of MCF-7 cells after incubation for 12 h. A: without additional C_B; B: with additional C_B.

and PEG-PTX was similar to each other, and there was no significant difference among each of them and the negative control ($p > 0.1$).

After C_B was added, all groups showed significantly more cells in G_2-M phase than the cell control (PEG-PTX: $p < 0.05$, PEG–VC–PABC–PTX: $p < 0.0005$). However, only the PEG–VC–PABC–PTX group with C_B showed a significant higher cell number of G_2-M phase than that without C_B ($p < 0.05$), while all other groups changed little (without significance), indicating that PEG–VC–PABC–PTX is significantly sensitive to C_B. For PEG-PTX, the cells in G_2-M phase still remained a relatively low level even in the presence of C_B.

Table 4
Effect of different treatments on the G_2-M phase (%) in cell cycle of MCF-7 cells incubated with or without C_B for 12 h ($n = 3$).

	Control (%)	PTX (%)	PEG-PTX (%)	PEG–VC–PABC–PTX (%)
G_2-M(without CB)	8.75 ± 1.60	41.91 ± 5.86[a]	21.15 ± 9.15	22.80 ± 9.26
G_2-M (with C_B)	7.82 ± 3.88	46.76 ± 2.88[c]	28.14 ± 7.61[b]	42.17 ± 1.10[c,d]

[a] $p < 0.001$ vs control.
[b] $p < 0.05$ vs control.
[c] $p < 0.0005$ vs control.
[d] $p < 0.05$ vs itself without C_B.

3.9. In vivo anti-tumor efficacy

The anti-tumor efficacy of two conjugates, PEG-PTX and PEG–VC–PABC–PTX was compared in animal experiment here, while the toxicities of these prodrugs were also evaluated by recording the changes in animal weight, as well as the animal status. As shown in Fig. 5, there was no anti-tumor efficacy observed in PEG-PTX group. However, compared to the 5% Glu and PEG-PTX group, the PEG–VC–PABC–PTX conjugate (equimolar with 10 mg/kg PTX) significantly inhibited the tumor growth ($p < 0.05$). All treatments showed no significant difference in body weight changes of animals (data not show), and the animal status in each test group was similar with the control group.

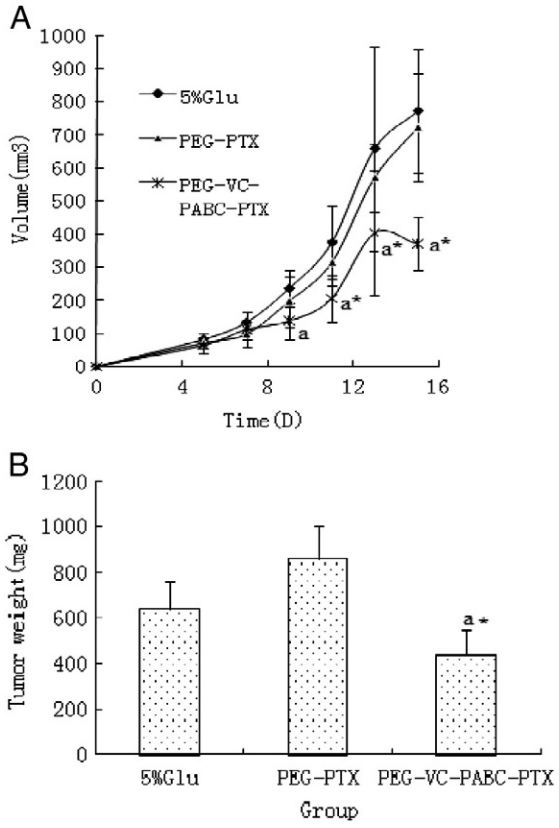

Fig. 5. Anti-tumor activity of different treatments in MCF-7 cells baring nude mice. (A) Tumor volume. (B) Tumor weight at the end of test. Treatment started when the average tumor size reached 80 mm^3 via tail vein every other day (n = 6). Animals were sacrificed on day 15 post-tumor inoculation. a, $p<0.05$ versus control; *, $p<0.05$ versus PEG-PTX.

Furthermore, various dosage of PEG–VC–PABC–PTX conjugate was compared with Taxol formulation, which is displayed in Fig. 6. Dramatic growth of tumor was observed in the 5% glucose group. Both Taxol formulation and PEG–VC–PABC–PTX (equimolar with 10 mg/kg PTX) conjugate showed a significant tumor inhibition in comparison with the control ($p<0.001$). Nevertheless, there was no significant difference in terms of therapeutic effect between Taxol formulation and PEG–VC–PABC–PTX conjugate ($p>0.5$) at the same dose of 10 mg/kg PTX. However, the Taxol formulation showed significant toxicity at this dose, evidenced by the most body weight loss and worst animal status, such as anorexia, lack of vitality, etc., preventing the further increase of drug dose. In contrast, the animals treated with PEG–VC–PABC–PTX (10 mg/kg PTX) demonstrated much less loss of body weight and much better status.

With the increase of dosage, the anti-tumor activity of the PEG–VC–PABC–PTX conjugate further improved. When the dose of PTX reached 20 mg/kg, this group exhibited significantly better antitumor effect than that of 10 mg/kg PTX group ($p<0.05$). It was observed that the body weight loss in PEG–VC–PABC–PTX (20 mg/kg PTX) group was similar to that of Taxol group (10 mg/kg PTX), while the animals in conjugate group were found with better vitality than that of Taxol group.

3.10. Effect on the angiogenesis, cell proliferation and toxicity in vivo

As shown in Fig. 7A, PEG–VC–PABC–PTX exhibited obvious antiangiogenesis effect, indicated by the lower density of tumor neovasculature compared with the negative control (5% Glucose), while PEG-PTX had no such effect at all. At the same dosage, there's no apparently

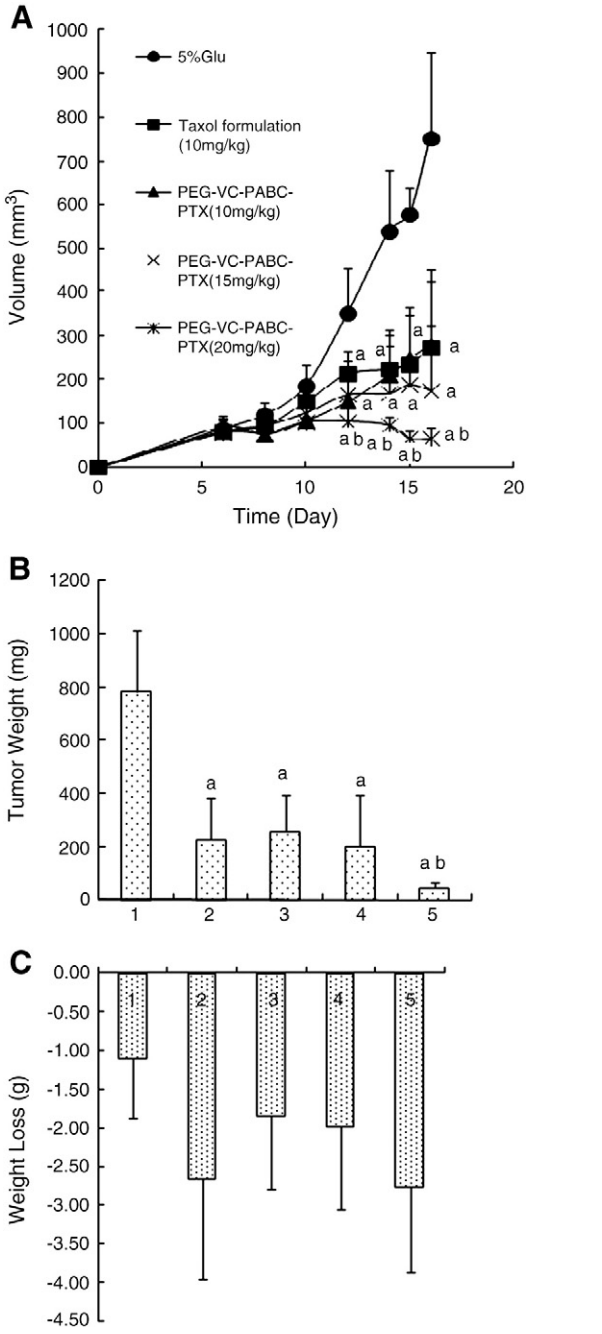

Fig. 6. Anti-tumor activity and body weight change of different treatments in MCF-7 cells baring nude mice. (A) Tumor volume. (B) Tumor weight at the end of test. (C) Body weight changed. Treatment started when the average tumor size reached 80 mm^3 via tail vein every other day (n = 6). Animals were sacrificed on day 17 post-tumor inoculation. (1) 5% glucose, (2) Taxol formulation (10 mg/kg), (3) PEG–VC–PABC–PTX (10 mg PTX/kg), (4) PEG–VC–PABC–PTX (15 mg PTX/kg), (5) PEG–VC–PABC–PTX (20 mg PTX/kg). a, $p<0.005$ versus control; b, $p<0.05$ versus Taxol formulation.

difference between Taxol and PEG–VC–PABC–PTX group, but the latter is slightly better than the former.

Fig. 7B presents the anti-proliferation effects of different treatments. Compared with the negative group, both Taxol formulation and PEG–VC–PABC–PTX could significantly inhibit tumor cell proliferation. However, no cell proliferation effect was observed in the PEG-PTX group.

Liver toxicity of different formulations is illustrated in Fig. 7C. After 5-time administration at the dosage of 10 mg PTX/kg, the two conjugates showed no apparent toxicity to mice liver. In contrast,

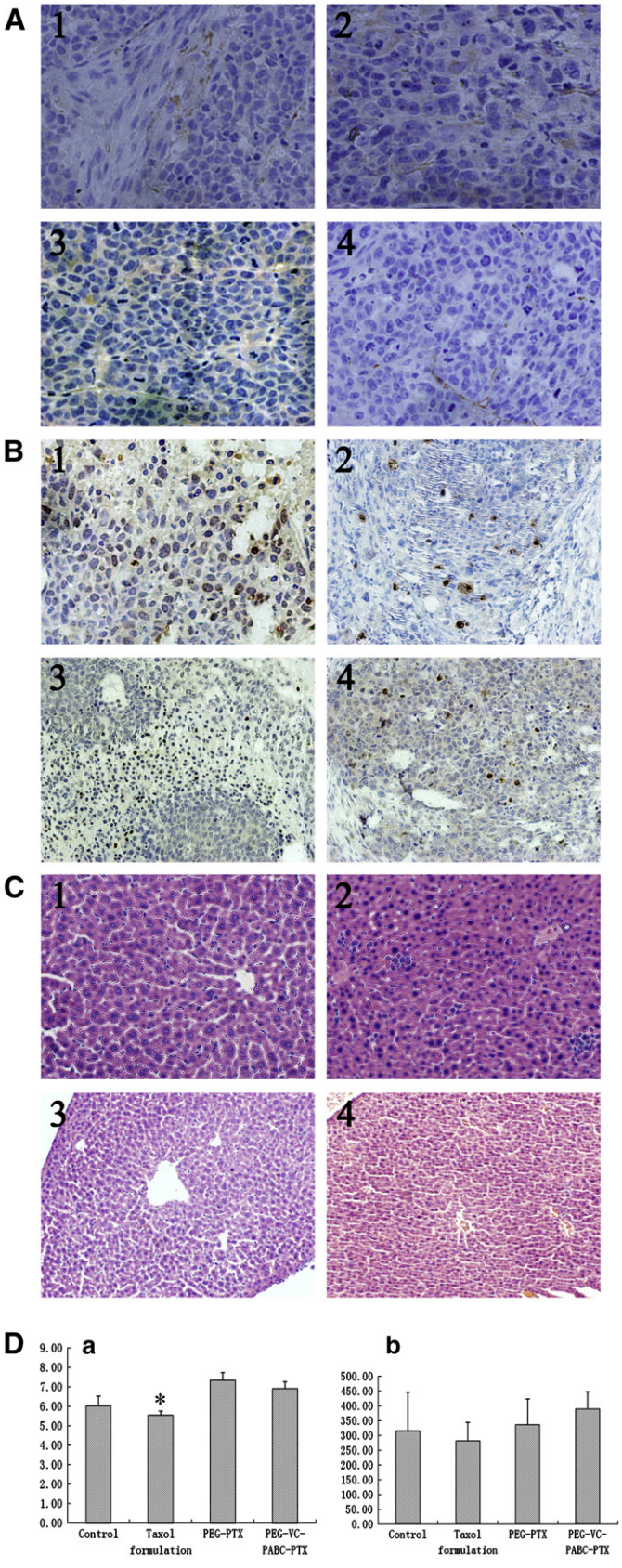

Fig. 7. Effect of various treatments on the angiogenesis, proliferation of tumors and in vivo toxicity. At the end of antitumor test in vivo, MCF-7 tumors were removed from mice with different treatments and sectioned. Tumor microvessel was stained by CD31 (Rabbit polyclonal antibody, Abcam, 1:200) and its proliferating cells were stained by Ki67 (Rabbit polyclonal antibody, Abcam, 1:200). The blood count was determined by a MEK-6318 K Hematology Analyzer (Nihon Kohden, Japan), and H&E staining of the liver tissue sections was conducted. (A) CD31; (B) Ki67; (C) Liver toxicity; (D) Hematotoxicity; (1) 5% glucose (negative control); (2) Taxol formulation (10 mg/kg); (3) PEG-PTX (equimolar to 10 mg/kg PTX); (4) PEG–VC–PABC–PTX (equimolar to 10 mg/kg PTX); (a) Hemoglobin concentration; (b) Platelet count; * $p<0.05$ vs 5% glucose group.

pyknosis can be observed in the Taxol group, indicating its effect on liver.

Moreover, platelet count and hemoglobin concentration are shown in Fig. 7D-a and D-b, respectively. None of the conjugates induced significant changes compared to negative control. However, Taxol formulation showed the lowest values among all treatment and also a significant inhibition on hemoglobin ($p<0.05$ vs negative control). The higher toxicity of Taxol formulation was likely due to the additives in its formulation.

4. Discussion

It is well known that the presence of Cremophore EL and ethanol (50/50, V/V) causes an array of severe adverse effects, which extremely narrow the use of PTX [37,38]. Without the use of Cremophore EL and ethanol, the two PTX conjugates prepared in this study will definitely have advantages over the present formulation of PTX injection (Taxol) in terms of less adverse effects if used in clinic, especially the hypersensitivity. Studies reveal that each PEG subunit is tightly associated with two or three water molecules [15], which make the conjugates water-soluble. PEG_{5000} was used here to provide enough PEG subunit, resulted in completed solubilization of highly insoluble PTX and a thousand time increase in the solubility. So, the second advantage of the two PTX conjugates here is their high solubility in water, saline or 5% glucose as seen in Table 1, which makes the preparation and use of PTX injection a very easy process.

In the design of our prodrugs, Val–Cit dipeptide was chosen as the linker because it was reported to be the most stable one under blood circulation (without C_B in blood) among several substrates of C_B [30]. PABC was also used as the spacer according to the previous report that drug will not release if dipeptide is directly connected to a drug, due to the lack of enough space for C_B to recognize [29]. It is supposed that PEG–VC–PABC–PTX conjugate may hydrolyze to PABC–PTX which is unstable and then quickly releases free PTX through spontaneous 1, 6-benzyl elimination and decarboxylation based on the chemical point of view [40,41].

The apparent particle size of each kind of conjugate was between 100 nm and 200 nm. Different from micelles with a mean particle size lower than 100 nm, conjugates were more likely to form the "nano-aggregation" when dissolved in aqueous phase, with a bigger inner core and a relatively large diameter (larger than 100 nm in average), which was previously reported [39]. At a given concentration of conjugates, some of them may aggregate while some of them may not aggregate, which was observed in TEM photograph of conjugates (Fig. 2). Here, the uniformity of particle size might be affected by the conjugate structure, molecular weight, concentration, preparation condition, and so on. The concentration of conjugates in DLS study (Table 2) was much high than that in TEM observation, which may cause greater fluctuation in particle size. These might be the reasons for the higher polydispersity.

As indicated in Fig. 3A, PEG-PTX released PTX faster than PEG–VC–PABC–PTX. This could be elucidated by the different structures between these two conjugates, ester bond for PEG-PTX and amide linkage for PEG–VC–PABC–PTX, namely, amide bond is more stable than ester bond.

It was also observed that even with C_B, the drug release from PEG–VC–PABC–PTX was not very fast (Fig. 3), possibly due to the steric hindrance of PEG at the condition of drug release. Because of the detectability of PTX by HPLC, we have to test the drug release at a rather high concentration of PEG–VC–PABC–PTX (800 nm/mL). At such high condition, the intense and long chains of PEG may interfere with the interaction of C_B with enzyme-sensitive linker. In the case of lower concentration of PEG–VC–PABC–PTX such as that in cell cycle test (20 nm/L), PEG–VC–PABC–PTX took effect within 12 h in the presence of C_B (Table 4), suggesting much easier interaction between C_B and the enzyme-sensitive linker. In vivo, the concentration of PEG–VC–PABC–PTX may not be high because of the dilution of blood.

As shown in Table 3, in vitro cytotoxicity study shows that the efficacy of PEG–VC–PABC–PTX was significantly lower than PTX ($p<0.0005$), while in vivo PEG–VC–PABC–PTX was found to be significantly effective than PTX (Taxol) at most of test points (Fig. 6). In vitro, free PTX could directly act on tumor cells while PEG–VC–PABC–PTX had to release PTX first then interact with tumor cells. Since conjugate release PTX slowly (Fig. 3), it was expected that free PTX showed better effect in vitro. However, the selectivity in drug release from the conjugate in tumor tissue in vivo was guaranteed by both EPR effect and C_B-sensitivity, while free PTX in vivo suffered from quick elimination, resulting in better efficacy of the C_B-sensitive conjugate.

It was noticed that the behaviors of the two conjugates were almost the same in cell tests in vitro, cytotoxicity or cell cycle test without C_B, though they released PTX differently in vitro. Firstly, this may be partially related to the different test conditions between drug release and cell tests, such as the shaking (100 rpm) in drug release study. In other words, PTX release from PEG-PTX may slow down in the condition of cell tests, narrowing the difference in drug release between these two conjugates. Secondly, in the tumor cell tests, the C_B sensitivity of PEG–VC–PABC–PTX is favorable for its effect on cells. All these facts may result in the similar effect of these two conjugates in cell tests in vitro.

As we know, PTX molecules exert their anti-tumor activity through the stabilization of microtubule assemblies, increase the fraction of cells in G_2-M phase, and thus interrupt mitosis and cellular division [35,36]. When MCF-7 cells were incubated with PEG–VC–PABC–PTX, cell number in G_2-M phase dramatically increased after C_B was added, while other groups changed little (Table 4 and Fig. 4). This study indicated that PEG–VC–PABC–PTX is C_B-sensitive and it works through the release of free PTX molecules. The C_B-sensitivity of PEG–VC–PABC–PTX had been proved again in sensitivity experiment as seen in Fig. 3B and C.

As seen in Fig. 4, it is obvious that PEG–VC–PABC–PTX conjugate showed the optimal anti-tumor efficacy in the two conjugates. This could be explained by their release properties and C_B sensitivity. In vivo, thanks to the PEGylation, both conjugates will not eliminate very faster in blood circulation, however, this is not the case for free drug. For PEG-PTX, it release free PTX faster than PEG–VC–PABC–PTX (Fig. 3), may leading to faster drug elimination in vivo and less drug accumulation into tumor tissue. Additionally, without the C_B sensitive linkage, PEG–PTX demonstrated no C_B sensitivity (Table 4), suggesting a non-specific drug distribution in vivo. On the other hand, the slow release of PTX from PEG–VC–PABC–PTX (Fig. 3) suggests a long circulation time of drug in vivo and more drug distribution in tumor. Furthermore, the C_B-sensitive conjugate may release more PTX than other groups in tumor tissue. As a result, a better anti-tumor efficacy was observed in the group of PEG–VC–PABC–PTX. On the other hand, based on the efficacy as well as toxicity (Fig. 6 and so on), it was clear that PEG–VC–PABC–PTX provides advantage over the current Taxol formulation with respect to therapeutic index.

As for the tumor model, typically, MCF-7 cells are estrogen-dependent and require ovariectomy and estrogen supplementation for predictable growth in vivo [42], although the biological properties of different MCF-7 cell lines may be different when derived from different sources [43]. By the way, Cremophor/ethanol was well understood for causing severe adverse effects but not for efficacy improvement, so they were not used as controls in the efficacy study.

For the body weight loss (Fig. 6C), there was no significant difference among all groups. The biggest difference in the average weight loss among all groups was about 5%. The reasons for this fact was not very clear, however, likely it was resulted from the large fluctuation frequently seen in animal test due to complicated factors. For instance, both tumor growth and drug treatment will cause body

weight loss, while antitumor drug may inhibit tumor growth. Similar situation was also found in previous report [44].

In the immunohistochemistry test (Fig. 7), PEG-PTX showed no anti-angiogenic or anti-proliferation effect at all, explaining why it exhibited no antitumor efficacy in vivo (Fig. 5). At the same dosage, effect of Taxol group and PEG–VC–PABC–PTX group was basically the same, which was also consistent to the result in anti-tumor test in vivo. .

It is also worthwhile to mention that site-specific property of a targeted DDS is relative. Especially, C_B is actually present in all cells including normal cells. So it is expected that some of conjugate will distribute into normal tissue, partially enter normal cells, even lysosomes, and consequently release free drug there.

5. Conclusion

A novel paclitaxel conjugate was designed and synthesized here. Compared with the control conjugate (PEG-PTX), PEG–VC–PABC–PTX was proved to be C_B-sensitive in terms of PTX release and its effect on cell cycle. Besides, this novel conjugate exhibited significant effects of antitumor, anti-angiogenesis and anti-proliferation in vivo, while the control conjugate was almost inefficacious at the same test. In comparison with PTX, the conjugates were very water soluble. Without Cremophore EL and ethanol, the conjugates will be certainly with less adverse effects. Moreover, the C_B-sensitive conjugate had a similar in vivo efficacy with the Taxol formulation, but much lower in vivo toxicity at the same doses. At the tolerant dose, however, PEG–VC–PABC–PTX showed significantly better antitumor efficacy than that of Taxol formulation. Therefore, design and application of a water-soluble and C_B-sensitive conjugate, like PEG–VC–PABC–PTX in this study, might be a potential strategy for the therapy with PTX.

Acknowledgment

This study was supported by projects from Ministry of Science and Technology, PR China (No. 2009CB930300 and No. 2009ZX09310-001) and National Science Foundation (No. 81130059).

References

[1] WorldHealthOrganization, Cancer, http://www.who.int/cancer/enAccessed July, 2010.
[2] I. Ojima, Guided molecular missiles for tumor-targeting chemotherapy-case studies using the second-generation taxoids as warheads, Acc. Chem. Res. 41 (1) (2008) 108–119.
[3] M.C. Wani, H.L. Taylo, M.E. Wall, P. Coggon, A.T. Mcphail, Plant antitumor agents. VI. The isolation and structure of taxol, a novel antileukemic and antitumor agent from *Taxus brevifolia*, J. Am. Chem. Soc. 93 (1971) 2325–2327.
[4] R.D. Dabholkar, R.M. Sawant, D.A. Mongayt, P.V. Devarajan, V.P. Torchilin, Polyethylene glycol-phosphatidylethanolamine conjugate (PEG-PE)-based mixed micelles: some properties, loading with paclitaxel, and modulation of P-glycoprotein-mediated efflux, Int. J. Pharm. 315 (2006) 148–157.
[5] A. Safavy, K.P. Raisch, M.B. Khazaeli, D.J. Buchsbaum, J.A. Bonner, Paclitaxel derivatives for targeted therapy of cancer: toward the development of smart taxanes, J. Med. Chem. 42 (1999) 4919–4924.
[6] X.F. Zhang, Y.X. Li, X.S. Chen, X.H. Wang, X.Y. Xu, Q.Z. Liang, J.L. Hu, X.B. Jing, Synthesis and characterization of the paclitaxel/MPEG-PLA block copolymer conjugate, Biomaterials 26 (2005) 2121–2128.
[7] X.D. Guo, J.P.K. Tan, S.H. Kim, L.J. Zhang, Y. Zhang, J.L. Hedrick, Y.Y. Yang, Y. Qian, Computational studies on self-assembled paclitaxel structures: templates for hierarchical block copolymer assemblies and sustained drug release, Biomaterials 30 (2009) 6556–6563.
[8] H. Ringsdorf, Structure and properties of pharmacologically active polymers, J. Polym. Sci. Symp. 51 (1975) 135–153.
[9] F. Greco, M.J. Vicent, Combination therapy: opportunities and challenges for polymer-drug conjugates as anticancer nanomedicines, Adv. Drug Deliv. Rev. 61 (2009) 1203–1213.
[10] J.W. Singer, S. Shaffer, B. Baker, A. Bernareggi, S. Stromatt, D. Nienstedt, M. Besman, Paclitaxel poliglumex (XYOTAX; CT-2103): an intracellularly targeted taxane, Anticancer Drugs 16 (2005) 243–254.
[11] T.M. Beer, C. Ryan, J. Alumkal, C.W. Ryan, J. Sun, K.M. Eilers, A phase II study of paclitaxel poliglumex in combination with transdermal estradiol for the treatment of metastatic castration-resistant prostate cancer after docetaxel chemotherapy, Anticancer Drugs 21 (2010) 433–438.
[12] C. Li, S. Wallace, Polymer-drug conjugates: recent development in clinical oncology, Adv. Drug Deliv. Rev. 60 (2008) 886–898.
[13] J.W. Singer, Paclitaxel poliglumex (XYOTAXTM, CT-2103): a macromolecular taxane, J. Control. Release 109 (2005) 120–126.
[14] M.J. Vicent, R. Duncan, Polymer conjugates: nanosized medicines for treating cancer, Trends Biotechnol. 24 (2006) 39–47.
[15] J.M. Harris, R.B. Chess, Effect of PEGylation on pharmaceuticals, Nat. Rev. Drug Discov. 2 (2003) 214–221.
[16] G. Pasut, F.M. Veronese, PEG conjugates in clinical development or use as anticancer agents: an overview, Adv. Drug Deliv. Rev. 61 (2009) 1177–1188.
[17] R.B. Greenwald, C.D. Conover, Y.H. Choe, Poly(ethylene glycol) conjugated drugs and prodrugs: a comprehensive review, Crit. Rev. Ther. Drug Carrier Syst. 17 (2000) 101–161.
[18] A. Nori, J. Kopecek, Intracellular targeting of polymer-bound drugs for cancer chemotherapy, Adv. Drug Deliv. Rev. 57 (2005) 609–636.
[19] D. Schmaljohann, Thermo- and pH-responsive polymers in drug delivery, Adv. Drug Deliv. Rev. 58 (2006) 1655–1670.
[20] G. Saito, J.A. Swanson, K.D. Lee, Drug delivery strategy utilizing conjugation via reversible disulfide linkages: role and site of cellular reducing activities, Adv. Drug Deliv. Rev. 55 (2003) 199–215.
[21] D. Filpula, H. Zhao, Releasable PEGylation of proteins with customized linkers, Adv. Drug Deliv. Rev. 60 (2008) 29–49.
[22] F.M. Veronese, O. Schiavon, G. Pasut, R. Mendichi, L. Andersson, A. Tsirk, J. Ford, G. Wu, S. Kneller, J. Davies, R. Duncan, PEG-doxorubicin conjugates: influence of polymer structure on drug release, in vitro cytotoxicity, biodistribution, and antitumor activity, Bioconjug. Chem. 16 (2005) 775–784.
[23] C.D. Conover, R.B. Greenwald, A. Pendri, K. Shum, Camptothecin delivery systems: the utility of amino acid spacers for the conjugation of camptothecin with polyethylene glycol to create prodrugs, Anticancer Drug Des. 14 (6) (1999) 499–506 (8).
[24] J.S. Mort, D.J. Buttle, Cathepsin B, Int. J. Biochem. Cell Biol. 29 (1997) 715–720.
[25] O. Vasiljeva, B. Turk, Dual contrasting roles of cysteine cathepsins in cancer progression: apoptosis versus tumour invasion, Biochimie 90 (2008) 380–386.
[26] H. Nishikawa, Y. Ozaki, T. Nakanishi, K. Blomgren, T. Tada, A. Arakawa, K. Suzumori, The role of cathepsin B and cystatin C in the mechanisms of invasion by ovarian cancer, Gynecol. Oncol. 92 (2004) 881–886.
[27] M. Devetzi, A. Scorilas, E. Tsiambas, M. Sameni, S. Fotiou, B.F. Sloane, M. Talieri, Cathepsin B protein levels in endometrial cancer: potential value as a tumor biomarker, Gynecol. Oncol. 112 (2009) 531–536.
[28] M.M. Mohamed, B.F. Sloane, Cysteine cathepsins: multifunctional enzymes in cancer, Nat. Rev. Cancer 6 (2006) 764–775.
[29] G.M. Dubowchik, R.A. Firestone, L. Padilla, D. Willner, S.J. Hofstead, K. Mosure, J.O. Knipe, S.J. Lasch, P.A. Trail, Cathepsin B-labile dipeptide linkers for lysosomal release of doxorubicin from internalizing immunoconjugates: model studies of enzymatic drug release and antigen-specific in vitro anticancer activity, Bioconjug. Chem. 13 (2002) 855–869.
[30] S.O. Doronina, B.E. Toki, M.Y. Torgov, B.A. Mendelsohn, C.G. Gerveny, D.F. Chace, R.L. DeBlanc, R.P. Gearing, T.D. Bovee, C.B. Siegall, J.A. Francisco, A.F. Wahl, D.L. Meyer, P.D. Senter, Development of potent monoclonal antibody auristatin conjugates for cancer therapy, Nat. Biotechnol. 21 (7) (2003) 778–784.
[31] S.C. Kim, J. Yu, J.W. Lee, E.S. Park, S.C. Chi, Sensitive HPLC method for quantitation of paclitaxel (Genexol®) in biological samples with application to preclinical pharmacokinetics and biodistribution, J. Pharm. Biomed. 39 (2005) 170–176.
[32] V. Vichai, K. Kirtikara, Sulforhodamine B colorimetric assay for cytotoxicity screening, Nat. Protoc. 1 (3) (2006) 1112–1116.
[33] Z. Wang, P.C. Ho, A nanocapsular combinatorial sequential drug delivery system for antiangiogenesis and anticancer activities, Biomaterials 31 (2010) 7115–7123.
[34] J.D. Liang, J. Liu, P. McClelland, M. Bergeron, Cellular localization of BM88 mRNA in paraffin-embedded rat brain sections by combined immunohistochemistry and non-radioactive in situ hybridization, Brain Res. Protoc. 7 (2001) 121–130.
[35] J.J. Manfredi, S.B. Horwitz, Taxol: an antimitotic agent with a new mechanism of action, Pharmacol. Ther. 25 (1) (1984) 83–125.
[36] J.F. Diaz, J.M. Andreu, Assembly of purified GDP-tubulin into microtubules induced by Taxol and Taxotere: reversibility, ligand stoichiometry, and competition, Biochemistry 32 (11) (1993) 2747–2755.
[37] W.Y. Seow, J.M. Xue, Y.Y. Yang, Targeted and intracellular delivery of paclitaxel using multi-functional polymeric micelles, Biomaterials 28 (2007) 1730–1740.
[38] R.T. Dorr, Pharmacology and toxicology of Cremophor EL diluent, Ann. Pharmacother. 28 (1994) S11–S14.
[39] H.S. Yoo, T.G. Park, Folate-receptor-targeted delivery of doxorubicin nano-aggregates stabilized by doxorubicin-PEG-folate conjugate, J. Control. Release 100 (2004) 247–256.
[40] R. Erez, E. Segal, K. Miller, R. Satchi-Fainaro, D. Shabat, Enhanced cytoxicity of a polymer-drug conjugate with triple payload of paclitaxel, Bioorg. Med. Chem. 17 (2009) 4327–4335.
[41] K.A. Ajaj, M.L. Biniossek, F. Kratz, Development of protein-binding bifunctional linkers for a new generation of dual-acting prodrugs, Bioconjug. Chem. 20 (2009) 390–396.
[42] S.E. Pratt, M.N. Pollak, Estrogen and antiestrogen modulation of MCF7 human breast cancer cell proliferation is associated with specific alterations in accumulation of insulin-like growth factor-binding proteins in conditioned media, Cancer Res. 53 (1993) 5193–5198.
[43] C.K. Osborne, K. Hobbs, J.M. Trent, Biological differences among MCF-7 human breast cancer cell lines from different laboratories, Breast Cancer Res. Treat. 9 (2) (1987) 111–121.
[44] S. Ning, K. Trisler, D.M. Brown, N.Y. Yu, S. Kanekal, M.J. Lundsten, S.J. Knox, Intratumoral radioimmunotherapy of a human colon cancer xenograft using a sustained-release gel, Radiol. Oncol. 39 (1996) 179–189.